Cell Transplantation, Vol. 22, pp. 2393–2408, 2013

0963-6897/13 $90.00 + .00
DOI: http://dx.doi.org/10.3727/096368912X658854
E-ISSN 1555-3892
www.cognizantcommunication.com

BMP2 Is Superior to BMP4 for Promoting Human Muscle-Derived Stem Cell-Mediated Bone Regeneration in a Critical-Sized Calvarial Defect Model

Xueqin Gao,*[1] Arvydas Usas,*[1] Aiping Lu,* Ying Tang,*† Bing Wang,*† Chien-Wen Chen,* Hongshuai Li,* Jessica C. Tebbets,* James H. Cummins,* and Johnny Huard*

*Stem Cell Research Center, Growth and Developmental Laboratory, Department of Orthopaedic Surgery, School of Medicine, University of Pittsburgh, Pittsburgh, PA, USA
†Molecular Therapy Laboratory, Department of Orthopaedic Surgery, School of Medicine, University of Pittsburgh, Pittsburgh, PA, USA

Muscle-derived cells have been successfully isolated using a variety of different methods and have been shown to possess multilineage differentiation capacities, including an ability to differentiate into articular cartilage and bone in vivo; however, the characterization of human muscle-derived stem cells (hMDSCs) and their bone regenerative capacities have not been fully investigated. Genetic modification of these cells may enhance their osteogenic capacity, which could potentially be applied to bone regenerative therapies. We found that hMDSCs, isolated by the preplate technique, consistently expressed the myogenic marker CD56, the pericyte/endothelial cell marker CD146, and the mesenchymal stem cell markers CD73, CD90, CD105, and CD44 but did not express the hematopoietic stem cell marker CD45, and they could undergo osteogenic, chondrogenic, adipogenic, and myogenic differentiation in vitro. In order to investigate the osteoinductive potential of hMDSCs, we constructed a retroviral vector expressing BMP4 and GFP and a lentiviral vector expressing BMP2. The BMP4-expressing hMDSCs were able to undergo osteogenic differentiation in vitro and exhibited enhanced mineralization compared to nontransduced cells; however, when transplanted into a calvarial defect, they failed to regenerate bone. Local administration of BMP4 protein and cell pretreatment with *N*-acetylcysteine (NAC), which improves cell survival, did not enhance the osteogenic capacity of the retro-BMP4-transduced cells. In contrast, lenti-BMP2-transduced hMDSCs not only exhibited enhanced in vitro osteogenic differentiation but also induced robust bone formation and nearly completely healed a critical-sized calvarial defect in CD-1 nude mice 6 weeks following transplantation. Herovici's staining of the regenerated bone demonstrated that the bone matrix contained a large amount of type I collagen. Our findings indicated that the hMDSCs are likely mesenchymal stem cells of muscle origin and that BMP2 is more efficient than BMP4 in promoting the bone regenerative capacity of the hMDSCs in vivo.

Key words: Human muscle-derived stem cells (hMDSCs); Lentiviral vector; Bone morphogenetic protein 2 (BMP2); Bone morphogenetic protein 4 (BMP4); Retroviral vector; Calvarial defect

INTRODUCTION

Healing of segmental bone defects and fracture nonunions pose a real challenge for clinical orthopedics; however, the development of new biological approaches that can address these hurdles is gaining momentum. Considerable progress toward repair or replacement of diseased or damaged bone tissue, using cell-based tissue engineering, has been made over the last decade. Bone marrow mesenchymal stromal (stem) cells (BMMSCs) have been considered an ideal autologous progenitor cell source for enhancing bone repair. It has been reported in clinical studies over the past decades that autologous human BMMSCs are highly effective, in combination with scaffolds, for the treatment of fracture nonunions, bone defects, and enhancing the effects of bone lengthening during distraction osteogenesis (6,16,23,40,42). In some situations, however, there are limitations with the availability of healthy bone marrow in patients; moreover, the harvesting procedure is invasive. The use of human adipose-derived stem cells has recently gained greater attention and has been shown to promote bone formation and bone defect healing in various animal models (2,8,21,27); however, their bone regenerative capacity is not optimal and has been hindered by

Received March 16, 2012; final acceptance October 18, 2012. Online prepub date: November 1, 2012.
[1]These authors provided equal contribution to this work.
Address correspondence to Dr. Johnny Huard, Stem Cell Research Center, Growth and Developmental Laboratory, Department of Orthopaedic Surgery, School of Medicine, University of Pittsburgh, Pittsburgh, PA 15219, USA. Tel: +1-412-648-2789; E-mail: jhuard@pitt.edu

several limitations (5,18,28). A recent study by Chou et al. demonstrated that human adipose stem cells could not improve segmental bone defect repair (4). It has also been demonstrated that rat adipose-derived stem cells readily form fat tissue compared to bone marrow-derived stem cells during the bone regeneration process (30); therefore, identifying other adult stem cell sources will provide additional options for future clinical applications.

Skeletal muscle tissue is easily accessible for orthopedic surgeons in the clinic. Human muscle-derived cells have been successfully isolated using a variety of different methods and have been shown to possess multilineage differentiation capacities. The migratory cells from human cranial facial muscles, selected using the surface marker CD56, can undergo myogenic, adipogenic, and osteogenic differentiation in vitro (41). In another study, Mastrogiacomo and colleagues isolated muscle-derived cells by selecting cells that adhered to the culture plate after 72 h in culture. These muscle-derived cells expressed vimentin, desmin, and α-sarcomeric actin and several osteogenic markers including alkaline phosphatase (AP), type I collagen, osteonectin, and osteopontin; moreover, they underwent adipogenic, chondrogenic, and osteogenic differentiation in vitro, and they could also form ectopic bone in vivo (31). More recently, it has been reported that muscle-derived cells that adhered to the culture plate after 24 h could be separated into two distinct populations, cluster of differentiation 56 positive ($CD56^+$) and $CD56^-$. Both populations expressed the mesenchymal stem cell markers CD73, CD90, CD105, CD44, and CD166 and were negative for the hemopoetic stem cell marker CD45. Interestingly, the $CD56^+$ cells expressed CD146, while the $CD56^-$ cells expressed CD15. The $CD56^+$ cells easily underwent myogenic differentiation, but their adipogenic differentiation capacity was limited. The $CD56^-$ cells underwent adipogenic differentiation with a limited myogenic differentiation capacity, although both populations could differentiate toward an osteogenic lineage (24). Myoendothelial cells isolated by flow cytometry based on their expression of $CD56^+CD34^+CD144^+CD146^-$ from human skeletal muscle have also been shown to be multipotent (47). It has also been shown that primary human muscle-derived cells transduced with adenoviral bone morphogenetic protein 2 (adeno-BMP2) or retroviral (retro)-BMP2 could induce ectopic bone formation and promote critical-sized calvarial defect healing in severe combined immunodeficient (SCID) mice (25,33); however, the osteogenic potential of human muscle-derived stem cells (hMDSCs) has not been broadly investigated, and their ability to regenerate bone has yet to be determined.

In this study, we isolated hMDSCs, which are likely the human counterparts of mouse muscle-derived stem cells and were found to highly express mesenchymal stem cell markers and undergo multipotent differentiation in vitro. Furthermore, we compared the effect that two different bone morphogenetic protein genes (BMP2 and 4) genetically constructed into two different viral vectors (lenti- and retroviral vectors, respectively) for their capacity to promote hMDSC bone regeneration. We constructed a retro-BMP2/4-green fluorescent protein (GFP) virus expressing BMP4 and GFP and a lenti-BMP2 virus expressing BMP2 in order to test their potential for hMDSC-mediated bone regeneration in combination with two different scaffolds, including fibrin sealant and Gelfoam. The retro-BMP2/4GFP-transduced hMDSCs did not induce bone formation within the critical-sized calvarial defects created in the two immunodeficient mouse strains using either of the scaffolds. In contrast, the lenti-BMP2-transduced hMDSCs displayed a remarkable bone regeneration capacity in vivo and nearly completely healed the calvarial bone defects created in CD-1 nude mice. Our findings suggest that BMP2 is more efficient than BMP4 in terms of its ability to promote the bone regenerative capacity of hMDSCs in vivo.

MATERIALS AND METHODS

Isolation of hMDSCs

Human skeletal muscle tissues obtained from two male donors (21 and 23 years old) and two female donors (30 and 76 years old) were purchased from the National Disease Research Interchange (NDRI, Philadelphia, PA, USA). All procedures were approved by the Institutional Review Board at the University of Pittsburgh. hMDSCs were isolated using a previously described modified preplate technique (14). Briefly, the human muscle tissues were cut into small pieces and subjected to collagenase type XI (Sigma-Aldrich, St. Louis, MO, USA) and dispase (Invitrogen, Darmstadt, Germany) digestion sequentially. The single cell suspensions were plated into flasks (BD Biosciences, Bedford, MA, USA). After 2 h, the floating cells were transferred to another flask (the adhering cells called pp1) and cultured for another 24 h. The floating cells (adhering cells called pp2) were then replated into another flask. The replating process was repeated for another four times every 24 h. After six times of replating, the floating cells were transferred to a new flask and cultured until all the cells eventually adhered to the flask. These cells are called preplate 6 cells (hMDSC). The cells were cultured in proliferation medium (PM) containing Dulbecco's modified Eagle's medium (DMEM), 20% fetal bovine serum (FBS; both from Gibco/Invitrogen, Carlsbad, CA, USA), 1% chicken embryo extract (Accurate Chemical and Scientific Corporation, Westbury, NY, USA), and 1% penicillin and streptomycin (Gibco). Cells were seeded at a density of 1,000 cells/cm^2, passaged every 3 days, and maintained at less than 50% confluence.

Surface Marker Expression of the hMDSCs

The marker profile of the cells from each donor was analyzed by flow cytometry. Briefly, cells at different passages (passages 6–13) were detached using trypsin–EDTA (Gibco), washed, and incubated with anti-human fluorochrome-conjugated antibodies: CD45-allophycocyanin (APC)-cyanine 7 (Cy7), CD56-phycoerythrin (PE)-Cy7, CD90-APC (1:100, all from Becton Dickinson, Franklin Lakes, NJ, USA), CD146-fluorescein isothiocyanate (FITC) (1:50, Serotec, Raleigh, NC, USA), CD44-PE (1:50, Becton Dickinson), CD73-PE, CD105-PE (1:50, both from Invitrogen, Carlsbad, CA, USA), and ligand *Ulexeuropaeus* agglutinin I (UEA-1-PE; 1:75, Biomeda, Foster City, CA, USA), for 20 min at 4°C and subsequently analyzed on a FACSAria flow cytometer (Becton Dickinson). Negative control samples received equivalent amounts of isotype-matched fluorophore-conjugated antibodies.

Stem Cell Gene Expression of the hMDSCs

The expression of stem cell genes POU class 5 homeobox 1 [POU5F1 or octamer-binding transcription factor 4 (OCT4)] and the Nanog homeobox (NANOG) and sex-determining region Y (SRY)-box 2 (SOX2) were tested using semiquantitative RT-PCR. RNA was extracted from nontransduced cells using Qiagen RNeasy mini kits (Qiagen, Dusseldorf, Germany). The cDNA was synthesized with a Superscript III cDNA synthesis kit (Invitrogen, Frederick, MD, USA) using 500 ng total RNA. The resultant cDNA was diluted with DNAase- and RNAase-free water (Promega Corporation, Madison, WI, USA) and kept at −20°C for further semiquantitative polymerase chain reaction (PCR) analysis. The PCR amplification of OCT4, NANOG, and SOX-2 were performed in a 25-μl reaction system using a Gotaq PCR kit (Promega). The PCR products were verified on a 1% agarose gel (Fisher Scientific, Fair Lawn, NJ, USA). The images were captured with a Bio-Rad Gel Doc system using QuantOne software (Bio-Rad, Hercules, CA, USA). Glyceraldehyde 3-phosphate dehydrogenase (GAPDH) was used as a loading control. Primer sequences are shown in Table 1.

Multipotent Differentiation Capacities of the hMDSCs

hMDSCs were tested for their myogenic, adipogenic, chondrogenic, and osteogenic differentiation capacities in vitro.

Myogenic Differentiation. Cells (6×10^4) were seeded in collagen-coated 12-well plates (Corning Inc., Corning, NY, USA). On the second day when the cells reached 100% confluence, the cells were shifted to myogenic medium, which contained high-glucose DMEM supplemented with 2% FBS and 1% penicillin/streptomycin. The medium was changed three times a week for a total of 2 weeks. Myogenic differentiation was determined via the use of antibodies against fast myosin heavy chain (fMHC, Sigma-Aldrich, Milwaukee, WI, USA; 1:400) and desmin (Sigma-Aldrich,1:20) using triple immunofluorescence staining with 4′,6-diamidino-2-phenylindoledihydrochloride (DAPI; Molecular Probes/Invitrogen, Eugene, OR, USA) as a nuclear stain.

Adipogenic Differentiation. Cells (2×10^5) were seeded in collagen-coated six-well plates (Corning). On the second day when the cells reached 100% confluence, the cells were shifted to adipogenic induction medium (Lonza, Walkersville, MD, USA) for 3 days and then

Table 1. Primer Information

Gene Name	Accession Number	Primers (5′–3′)	Product Size (bp)	Annealing Temperature (°C)
SOX-9	NM_000346.3	F: GCTCAGCAAGACGCTGGGCA R: CCGGAGGAGGAGTGTGGCGA	249	55
BMPR1B	NM_001203.2	F: AGGCCTCCCTCTGCTGGTCC R: TTCGCCACGCCACTTTCCCA	108	55
BMPR2	NM_001204.6	F: TCCCATGCTGCCACAACCCA R: TGGCCGTTCCCTCCTGTCCA	231	55
COX-2	NM_000963.2	F: GCGAGGGCCAGCTTTCACCA R: CCTGCCCCACAGCAAACCGT	225	55
NANOG	NM_024865.2	F: TTCCTTCCTCCATGGATCTG R: TCTGCTGGAGGCTGAGGTAT	213	58
OCT4	NM_002701.4	F: AGTGAGAGGCAACCTGGAGA R: GTGAAGTGAGGGCTCCCATA	273	58
SOX-2	NM_003106.3	F: CACAACTCGGAGATCAGCAA R: GTTCATGTGCGCGTAACTGT	294	58
GAPDH	NM_002046.4	F: GCCTTCCGTGTCCCCACTGC R: CAATGCCAGCCCCAGCGTCA	211	58

F, forward; R, reverse; SOX-9, sex-determining region Y box 9; BMPR1B, bone morphogenetic protein receptor 1B; COX-2, cyclooxygenase-2; OCT4, octamer-binding transcription factor 4; GAPDH, glyceraldehyde 3-phosphate dehydrogenase.

switched to adipogenic maintenance medium (Lonza) for 2 days. The noninduced control was cultured in adipogenic maintenance medium for the entire period of culture. After three cycles of induction, the cells were cultured in adipogenic maintenance medium for another 7 days. Adipogenic differentiation was determined by oil red O (Sigma-Aldrich) staining.

Chondrogenic Differentiation. Cells (2.5×10^5) were aliquoted into 15-ml tubes (BD Biosciences), after centrifugation at $800 \times g$ for 5 min, the cells were resuspended in chondrogenic basal medium (Lonza) and centrifuged again. The cells were then resuspended in complete chondrogenic medium [chondrogenic basal medium supplemented with 10 ng/ml transforming growth factor β3 (Invitrogen)] and centrifuged at $500 \times g$ for 5 min. Cell pellets were maintained in chondrogenic medium for 21 days with medium change three times a week. Chondrogenic differentiation was verified by Alcian blue staining (http://www.ihcworld.com/_protocols/special_stains/alcian_blue.htm).

Osteogenic Differentiation. We also utilized pellet cultures for the osteogenic differentiation assay. Cells (2.5×10^5) were aliquoted into each 15-ml tube, centrifuged, resuspended in osteogenic medium containing high-glucose DMEM supplemented with 10% FBS, 1% penicillin/streptomycin, 10^{-2} M β-glycerol phosphate, 50 μg/ml L-ascorbic acid-2 phosphate, and 10^{-7} M dexamethasone (all Sigma-Aldrich unless previously specified), and centrifuged at $500 \times g$ for 5 min. Pellets were subjected to medium changes three times a week. The pellets were monitored by microcomputed tomography (microCT; Viva CT40; Scanco Medical, Scanco USA Inc., Wayne, PA, USA) every week for 4 weeks to evaluate mineralized matrix deposition. After 4 weeks, pellets were embedded in NEG50 freezing medium (Thermo Scientific, Kalamazoo, MI, USA) and snap frozen in liquid nitrogen, and 8-μm sections were cut and fixed for 10 min in 10% neutral buffered formalin (Sigma-Aldrich). Mineralization was detected by von Kossa staining using an online protocol (http://www.ihcworld.com/_protocols/special_stains/von_kossa.htm). Osteocalcin (MAB1219, 1:100; R&D Systems, Minneapolis, MN, USA) immunohistochemistry was performed to validate osteogenic differentiation. Diaminobenzidine (DAB) staining kit (Vector Laboratories, Burlingame, CA, USA) was used to reveal the osteocalcin-positive cells. Hematoxylin QS (Vector Laboratories Inc.) was used to counterstain nuclei.

Construction of Retro-BMP2/4GFP, Cell Transduction, In Vitro Osteogenic Differentiation, and Gene Expression Analysis

Retro-BMP2/4GFP was constructed as previously described (37,38). The BMP4 signal peptide sequence in this construct was replaced with the BMP2 signal peptide to increase the secretion level of the recombinant protein (36). The GFP tag was inserted downstream of the BMP4 gene with an internal ribosome entry site to allow the target gene BMP4 and the tag gene GFP to be expressed as separate proteins. hMDSCs were transduced with retro-BMP2/4GFP at a multiplicity of infection (MOI) of 5 in the presence of 8 μg/ml of polybrene (Sigma-Aldrich). The viral transduction was repeated three times at 12-h intervals. The transduced cells were expanded, and their transduction efficiency was evaluated by GFP expression observed via fluorescence microscopy. At passage 4 posttransduction, the cells were sorted [fluorescence-activated cell sorting (FACS), BD FACSAria IIu, Bedford, MA, USA] to obtain cells that were 100% positive for GFP expression in order to track the donor cells in vivo. The BMP4 secretion level was measured using a Human BMP-4 Quantikine ELISA Kit (R&D Systems) and expressed as the mean ± SD ng/million cells/24 h. A pellet culture assay was used to evaluate the osteogenic potential of both transduced and nontransduced hMDSCs as described above in vitro. To identify the genes that might be associated with the osteogenic differentiation potential of the hMDSCs, RT-PCR for the Sry box-9 gene (SOX-9), bone morphogenetic protein receptor 1B (BMPR1B), bone morphogenetic protein receptor 2 (BMPR2), and cyclooxygenase 2 (COX-2) were performed using the methods described above. The primer sequences are shown in Table 1.

Transplantation of Retro-BMP2/4GFP-Transduced hMDSCs Into a Calvarial Bone Defect

All animal protocols were approved by the Institutional Animal Care and Use Committee of the University of Pittsburgh. Three immunocompromised animal models, B6 SCID, SCID-beige, and CD-1 nude mice, were used to evaluate whether the strain of the host animal affected the bone regeneration capacity of the hMDSCs. Retro-BMP2/4GFP-transduced hMDSCs were trypsinized, resuspended in phosphate-buffered saline (PBS) to a final concentration of 1.5×10^6/10 μl and seeded on Gelfoam (Ethicon, Somerville, NJ, USA) that has been cut into 6 mm × 6 mm pieces and placed into a 24-well plate. After the cell suspension completely soaked into the Gelfoam, 1 ml of PM was added to each well, and the plate was incubated overnight in 5% CO_2 at 37°C. Male B6 SCID mice (Jackson Laboratory, Bar Harbor, ME, USA) were randomly divided into three groups ($n = 4$). Animals in group 1 received 1.5×10^6 retro-BMP2/4GFP-transduced hMDSCs using Tisseel fibrin sealant including thrombin and fibrinogen (Baxter Healthcare Corporation, Westlake Village, CA, USA) scaffold, group 2 received 1.5×10^6 retro-BMP2/4GFP-transduced hMDSCs seeded in Gelfoam, and group 3 received 5×10^5 retro-BMP4GFP-transduced murine muscle-derived stem cells [mMDSCs; obtained from C57BL/10J mice (Jackson Laboratory)

using previously described protocol], which served as a positive control using Tisseel fibrin sealant scaffold. Critical-sized 5-mm-diameter calvarial (skull) defects were created in mice under general inhalation anesthesia (3% isoflurane and oxygen) using a trephine (Fine Science Tools, Foster City, CA, USA) after removing the periosteum. When using Tisseel fibrin sealant, 10 µl of the cells combined with 15 µl of thrombin was applied to the bone defect first, and then 15 µl of fibrinogen was added, allowing 1 min for it to solidify before wound closure with sutures (Ethicon LLC, Johnson Johnson, San Lorenzo, Puerto Rico). The Gelfoam scaffolds seeded with cells were gently rinsed in PBS and applied to the defect followed by wound closure with sutures. Bone regeneration was monitored by microCT at 2, 4, and 6 weeks postimplantation. After 6 weeks, the animals were sacrificed, and skull tissues were harvested, snap frozen in NEG50 medium with liquid nitrogen, and stored at −80°C.

In another set of experiments, we either applied 500 ng of BMP4 protein (R&D Systems) locally or treated the retro-BMP2/4GFP-transduced hMDSCs before transplantation with *N*-acetylcysteine (NAC, Sigma-Aldrich) to enhance cell survival. In short, retro-BMP2/4GFP-transduced hMDSCs were cultured in PM and expanded. NAC was added to the flasks at a concentration of 10 mM, and cells were allowed to grow for another 24 h. Both treated and untreated cells were trypsinized, washed, and resuspended in PBS to a final concentration of 1.5×10^6 cells/10 µl. Eight-week-old male CBGCBS SCID mice (C.B-Igh-1b/GbmsTAC-PrkdcSCID, aka SCID/Beige, Taconic, Hudson, NY, USA) were divided into the following three groups ($n = 4$): group 1 received 500 ng BMP4 + Tisseel fibrin sealant; group 2 received retro-BMP2/4GFP-transduced hMDSC + 500 ng BMP4 + Tisseel fibrin sealant; and group 3 received NAC-treated retro-BMP2/4GFP-transduced hMDSC + 500 ng BMP4 + Tisseel fibrin sealant. Animal surgery was performed as previously described, and the healing of the bone defect was monitored biweekly by microCT for 8 weeks. The mice were then sacrificed, and the skulls were processed for histological evaluation. Some animals in group 2 were sacrificed at day 7 and day 21 posttransplantation to investigate cell survival. Dual-color immunofluorescence was used to detect the infiltration of neutrophils using rat anti-granulocyte receptor-1 (Gr-1) antibody (1:100 dilution, BD Bioscience, San Jose, CA, USA) and vascular endothelial cells using rat anti-CD31 antibody (1:300 dilution, BD Bioscience) and colocalized with rabbit anti-GFP antibody (Ab290, Abcam, Cambridge, MA, USA). Donkey anti-rat-594 and donkey anti-rabbit-Cy2 secondary antibodies (Jackson Immunoresearch Laboratory, West Grove, PA, USA) were used to reveal Gr-1 and CD31, and GFP, respectively. Nuclear counter staining was performed using DAPI.

Evaluation of the Effect of BMP4 Stimulation on hMDSC Proliferation

In order to investigate whether BMP4 could affect the proliferation of hMDSCs, we performed an in vitro proliferation assay. Two thousand cells were plated in each well of a 24-well plate. A recombinant human BMP4 (rhBMP4; R&D Systems) stock solution was prepared according to the manufacturer's directions in order to achieve final concentrations of 100, 50, 25, and 0 ng/ml. Cells were cultured in PM as stated above. For the 3-day stimulation experiment, rhBMP4 was added on day 1. For the 5-day stimulation experiment, the same amount of rhBMP4 was added on days 1 and 3. C2C12 murine myoblast cell line (ATCC, Manassas, VA, USA) was used as a positive control to test the bioactivity of the rhBMP4 protein. After stimulation, the cells were washed with PBS, and the DNA content was measured using a Quant-iT™ Picogreen double-stranded DNA (dsDNA) assay kit (Molecular Probes/Invitrogen). Briefly, cells in each well were lysed in 200 µl of 0.1% Triton X-100 (Sigma-Aldrich) for 20 min, incubated at 37°C for 10 min, and then homogenized well by pipetting. The cells were kept at −80°C for 2 h, mixed, and incubated at 37°C for another 10 min. Fifty microliters of the cell lysate was transferred to a nontransparent 96-well plate (Becton Dickson & Company, Franklin Lakes, NJ, USA), and 50 µl of Tris-EDTA (TE; Sigma-Aldrich) buffer and 100 µl Picogreen were added following incubation for 10 min. The fluorescent intensity was measured via a plate reader (Tecan Infinite M200, Männedorf, Switzerland). Fluorescent intensity represents the amount of double-stranded DNA that correlates to the cell number. Alkaline phosphatase (AP) staining was performed using 86C kit (Sigma-Aldrich) to test for osteogenesis.

Construction of the Lenti-BMP2 Vector, Transduction of hMDSCs, and In Vitro Osteogenic, Chondrogenic, and Myogenic Differentiation After Transduction

The human BMP2 gene in the lentiviral vector was under the control of the human cytomegalovirus (CMV) promoter. An SV40 early promoter was inserted downstream of the BMP2 expression cassette to drive a higher level of constitutive expression of an antibiotic resistance gene, which allowed for the use of blasticidin (Gibco/Invitrogen) to select the BMP2-transduced positive cells. Lenti-BMP2 virus was packaged using 293T cells (ATCC). The hMDSCs were first expanded in PM until they reached 30% confluence and then transduced with lenti-BMP2 virus (diluted 1:1 with PM) for 16 h in the presence of 8 µg/ml of polybrene. The transduced cells were allowed to recover in PM for 24 h. At this time, we collected the supernatant to quantify BMP2 secretion levels (Quantikine BMP2, R&D Systems). The transduced cells were then selected by adding 10 µg/ml of blasticidin (Invitrogen, Life Technologies) for a 48-h period. After selection, the

cells were cultured in PM, and the supernatant from passages 1, 3, and 5 after blasticidin selection (BLP1-5) was collected to measure BMP2 secretion levels, which were normalized to ng/million cells/24 h. In addition, AP staining was performed as stated above. In vitro osteogenic pellet culture, chondrogenic pellet culture, myogenic differentiation assays, and RT-PCR were also performed for the lenti-BMP2-transduced hMDSCs and compared to the nontransduced cells, as described above.

Transplantation of Lenti-BMP2-Transduced hMDSCs Into a Calvarial Defect in CD-1 Nude Mice

Male CD-1 nude mice (Charles River Laboratories, Wilmington, MA, USA) were divided into three groups ($n = 4$). Animals in group 1 received fibrin sealant + 10 µl of PBS; animals in group 2 received fibrin sealant + 1.5×10^6 retro-BMP2/4GFP transduced-hMDSCs in PBS; animals in group 3 received fibrin sealant + 1.5×10^6 lenti-BMP2-transduced hMDSCs in PBS. New bone formation in the defect area was monitored by microCT biweekly for 6 weeks. Mice were then sacrificed, and the skulls were harvested and fixed in 10% neutral buffered formalin, decalcified with 10% EDTA (Fisher Scientific) plus 1% sodium hydroxide (Fisher Scientific) for 2 weeks, and embedded in paraffin. Herovici's polychrome staining using 0.05% w/v acid fuchsin in picric acid (Sigma Aldrich) and 0.05% w/v methyl blue (Sigma Aldrich) in 1% acetic acid v/v (Sigma Aldrich) was performed to identify type I collagen-positive bone matrix formation as described in the literature (26,39,43). Images were captured with a Nikon microscope (Nikon, Melville, NY, USA) equipped with a Retiga digital camera using Q Capture software (Q Imaging, Inc., Surrey, BC, Canada).

Microcomputed Tomography Analysis

Bone regeneration within the calvarial bone defect was monitored using microcomputed tomography that was performed biweekly after surgery. After obtaining two-dimensional image slices of the skulls, the view of interest (VOI) was uniformly delineated. Three-dimensional reconstructions were created using an appropriate threshold that was kept constant throughout the analyses. The newly regenerated bone volume was measured using evaluation software provided by the manufacturer. The bone morphometry including volume (mm^3) and density [milligrams hydroxyapatite per cubic centimeter (mg HA/cm^3)] measurements regarding the nomenclature, symbols, and units followed the guidelines set by the American Society of Bone and Mineral Research (3). The bone defect area was measured with Image J software (http://rsbweb.nih.gov/ij/), and the percentage of bone healing was determined by dividing the area covered by the newly regenerated bone after 2, 4, and 6 weeks posttransplantation by the original defect area measured on day 1.

Statistical Analysis

All quantitative data are expressed as the mean ± standard deviation. Student's t test was used for comparison between the two groups. Analysis of variance (ANOVA) and Tukey's HSD post hoc test was used for multigroup comparison. A value of $p < 0.05$ was considered statistically significant.

RESULTS

Characterization of hMDSCs

hMDSCs isolated by a modified preplate technique were characterized by flow cytometry for several cell lineage markers, including CD45 (leukocytes/hematopoietic cells), CD56 (myogenic cells), Ulexeuropaeus agglutinin I receptor (UEA-1R, endothelial cells), CD146 (pericytes/endothelial cells), as well as classic mesenchymal stem/stromal cell (MSC) markers: CD44, CD73, CD90, and CD105. We found that hMDSCs robustly expressed CD56, CD146, and all four MSC markers (more than 99% positive) but not CD45 or UEA-1R (Fig. 1A). Quantitative analysis revealed a consistent marker expression profile in all the hMDSC populations examined (Fig. 1B). RT-PCR results revealed that cells from all donors expressed the stem cell markers OCT4 and NANOG, while cells from two of the donors (23-year-old male and 76-year-old female) slightly expressed SOX-2 (Fig. 1C). In vitro differentiation assays indicated that the hMDSCs could undergo adipogenic, chondrogenic, osteogenic, and myogenic differentiation as shown by oil red O staining, Alcian blue staining, von Kossa staining, and fMHC and desmin immunofluorescence, respectively (Fig. 1D).

Retro-BMP2/4GFP Transduction Efficiency and In Vitro Osteogenesis

The map of the retro-BMP2/4GFP construct is shown in Figure 2A. The BMP4 signal peptide sequence was replaced with the BMP2 signal peptide to enhance the secretion level of BMP4. Detailed information regarding the retro-BMP4GFP vector is shown in Table 2. The transduction efficiency of the hMDSCs was approximately 50%. After FACS, 100% of the cells were GFP positive (Fig. 2B). The BMP4 secretion level, measured by ELISA, was 6.19 ± 1.4 ng/million cells/24 h. Nontransduced hMDSCs had no detectable BMP4 secretion. The mRNA expression levels of the *SOX-9*, *BMPR1B*, *BMPR2*, and *COX-2* genes did not change after transduction with retro-BMP2/4GFP (Fig. 2C). We did not observe any AP-positive cells before or after transduction (data not shown). MicroCT analysis of the cell pellets cultured in osteogenic medium revealed that both nontransduced and retro-BMP2/4GFP-transduced hMDSCs underwent mineralization in vitro. Retro-BMP2/4GFP-transduced hMDSCs began to deposit a calcified matrix at 1 week, and the mineralized pellet volume in this group was

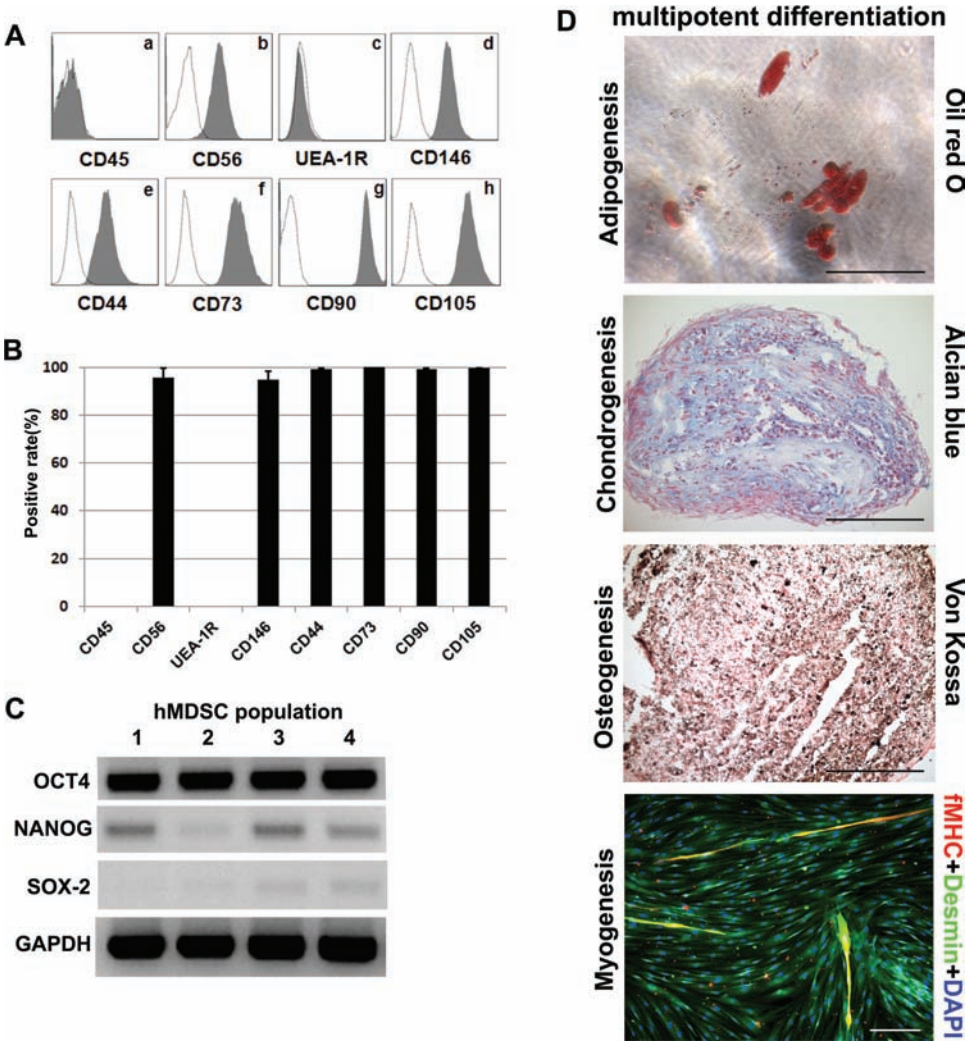

Figure 1. Characterization of the human muscle-derived stem cells (hMDSCs). (A) Flow cytometry analysis of hMDSC surface markers revealed robust expression of cluster of differentiation 56 (CD56), CD146, CD44, CD73, CD90, and CD105 but not CD45 or *Ulexeuropaeus* agglutinin I receptor (UEA-1R). (B) Quantification of cell lineage marker expression in hMDSCs from four donors demonstrated consistency in their cell marker expression profiles. (C) RT-PCR results of stem cell markers. Cells from each donor expressed the stem cell markers octamer-binding transcription factor 4 (OCT4) and NANOG, but only a faint expression of sex-determining region Y box-2 (SOX-2) was detected in cells from two donors (3 and 4). Glyceraldehyde 3-phosphate dehydrogenase (GAPDH) was used as a loading control. (D) Multipotent differentiation of hMDSCs. hMDSCs undergo adipogenesis (oil red staining), chondrogenesis (Alcian blue staining), osteogenesis (von Kossa staining), and myogenesis as shown by fast myosin heavy chain (fMHC) and desmin immunofluorescence. Scale bars: 200 μm.

significantly higher compared to the nontransduced cell group at each time point (Fig. 2D). The pellet density was also significantly higher in the transduced cell group at 1 and 2 weeks, but there was no difference between the two groups after 3 weeks. von Kossa staining and human osteocalcin immunohistochemistry revealed bone matrix formation in both pellet groups (Fig. 2E). These results suggest that the hMDSCs can undergo osteogenic differentiation in vitro and that retro-BMP2/4GFP transduction can enhance the osteogenic potential of the hMDSCs.

Retro-BMP2/4GFP-Transduced hMDSCs Failed to Regenerate Bone In Vivo

We further investigated whether the retro-BMP2/4GFP-transduced hMDSCs could regenerate bone tissue in vivo and heal a critical-sized calvarial defect. Retro-BMP2/4GFP-transduced hMDSCs delivered with either fibrin sealant or Gelfoam scaffold showed only negligible bone regeneration at 6 weeks, as demonstrated by microCT. In contrast, mMDSCs transduced with retro-BMP4GFP (BMP4 secretion level 19.1 ng/million/24 h),

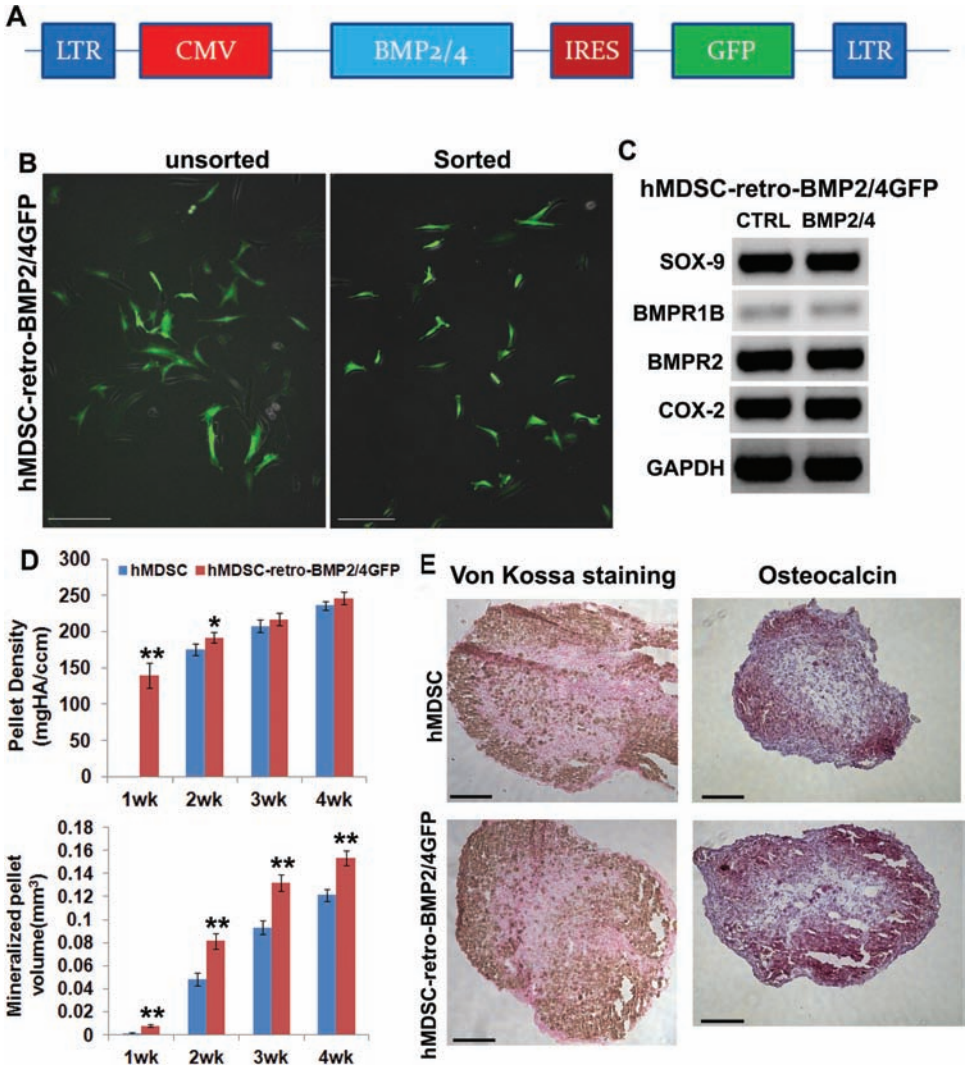

Figure 2. Osteogenic differentiation of hMDSCs and retro-BMP2/4GFP-transduced hMDSCs in vitro. (A) Schematic illustration of the retro-bone morphogenetic protein 2/4 green fluorescent protein (BMP2/4GFP) vector. (B) The 100% GFP-positive retro-BMP2/4GFP-transduced hMDSCs were obtained by fluorescence-activated cell sorting (FACS). Scale bars: 200 μm. (C) RT-PCR results indicated no significant gene expression changes before and after retro-BMP2/4GFP transduction of the hMDSCs. (D) Microcomputed tomography (microCT) evaluation of matrix mineralization of retro-BMP2/4GFP-transduced and nontransduced hMDSCs in the osteogenic pellet culture assay. $^{**}p < 0.01$ compared to nontransduced hMDSCs ($n = 4$). (E) von Kossa staining of the pellets at 4 weeks showed that both transduced and nontransduced hMDSCs underwent osteogenesis. Osteocalcin staining indicated the differentiation of hMDSCs into osteogenic lineage. Scale bars: 100 μm. LTR, long terminal repeat; CMV, cytomegalovirus; IRES, internal ribosome entry site; BMPR1B, bone morphogenetic protein receptor 1B; COX-2, cyclooxygenase-2; mg HA/cm^3, mg hydroxyapatite per cubic cm.

which served as a positive control, were able to completely heal the defect after 4 weeks (Fig. 3A).

In order to further investigate the inability of the retro-BMP2/4GFP-transduced hMDSCs to form bone in vivo, we performed additional experiments in which we used CBSCBG SCID mice that are not only deficient in T-cells but also lack macrophages and NK cells (http://www.taconic.com/wmspage.cfm?parm1=1324), instead of using SCID mice. In addition, we attempted to boost the osteogenic potential of the transplanted cells and enhance cell survival. In one group of animals, 500 ng of rhBMP4 protein was applied locally to the defect site at the time of retro-BMP2/4GFP-transduced hMDSC transplantation. A second group of animals received retro-BMP2/4GFP-transduced hMDSCs that were treated in vitro with NAC to enhance cell survival. Surprisingly, we did not observe bone formation in any of the treatment groups as well as the BMP4-only group even after 8 weeks postimplantation (Fig. 3B). Immunofluorescent staining performed on regenerated tissue samples obtained from animals sacrificed at 7

Table 2. Comparison of Retro-BMP2/4GFP, Retro-BMP4GFP, and Lenti-BMP2 Vectors

	Retro-BMP2/4GFP	Retro-BMP4GFP	Lenti-BMP2
Vector	Retrovirus	Retrovirus	Lentivirus
Expression of target gene	BMP4 and GFP	BMP4 and GFP	BMP2
Promoter	CMV	CMV	CMV
Signal peptide	BMP2	BMP4	BMP2
Transduction	Infection in the presence of polybrene (8 μg/ml)	Infection in the presence of polybrene (8 μg/ml)	Infection in the presence of polybrene (8 μg/ml)
Infection time	3 times in 36 h	3 times in 36 h	1 time in 16 h
Selection method	GFP-based flow cytometry cell sorting	GFP-based flow cytometry cell sorting	Blasticidin 10 μg/ml for 24 h
Amount of protein expressed (ng/million cells/24 h)	6 ng of BMP4 in hMDSC	20 ng of BMP4 in mouse MDSC	2.8 ng of BMP2 in hMDSC
Persistency of expression overtime	Stable for about 15 passages after cell sorting	Stable for about 15 passages after cell sorting	Relatively stable and have a trend to decrease overtime
Number of transplanted cells	1.5×10^6	0.5×10^6	1.5×10^6
In vivo efficacy to promote bone regeneration	No healing in defect with hMDSC	Completely healed the defect with mMDSC	70–80% healed the defect area with hMDSC

GFP, green fluorescent protein; CMV, cytomegalovirus; hMDSC, human muscle-derived stem cell.

and 21 days after surgery demonstrated that GFP-positive donor cells (green) were still present within the defect area 7 days after implantation. At the same time, we also observed Gr-1-positive neutrophil infiltration and the presence of CD31 vascular endothelial cells, which were of host origin. von Kossa staining of the samples obtained at 21 days posttransplantation revealed some scattered mineralization in the defect area, but the regenerated tissues were predominantly composed of granulation tissue. Immunofluorescent staining revealed very few GFP-positive donor-derived cells, even though host-derived CD31-positive vascular cells were detected in the defect area (Fig. 3C). These results indicated that the donor cells were unable to survive and induce bone formation.

The Effect of BMP4 Stimulation on Proliferation and Differentiation of hMDSCs

In order to test whether BMP4 protein had an adverse effect on the hMDSCs, we investigated the proliferation and differentiation capacity of the hMDSCs after stimulation with rhBMP4 in vitro. We found an increase in the hMDSC proliferation after 3 days when the cells were stimulated with 50 or 100 ng/ml of BMP4 protein on day 1 (Fig. 4A). In contrast, when BMP4 protein was applied on days 1 and 3, the hMDSC proliferation rate decreased in all groups after 5 days in culture, with the greatest reduction in proliferation occurring in the 100-ng/ml group (Fig. 4B). In order to evaluate the osteogenic differentiation capacity of the hMDSCs after BMP4 stimulation, we performed AP staining at 3 and 5 days and found that, regardless of the BMP4 dose, the cells did not express AP at any time point (Fig. 4C). C2C12 myoblasts were used as a positive control and demonstrated AP-positive staining after stimulation with 25 and 50 ng/ml of BMP4 protein for 3 days (Fig. 4D).

Lenti-BMP2-Transduced hMDSCs Exhibited an Enhancement of Osteogenic and Chondrogenic Differentiation but Did Not Undergo Myogenic Differentiation In Vitro

Lentivirus can infect not only dividing cells but also nondividing cells; therefore, we constructed a lentiviral vector with a full-length human BMP2 gene under the control of a CMV promoter. The map and detailed information about the lenti-BMP2 construct are shown in Figure 5A and Table 2. ELISA results revealed that the BMP2 secretion level was 547 ng/million cells/24 h at 24 h after hMDSC transduction (data not shown). The BMP2 secretion level after blasticidin selection at passage 1 was 18.06 ng/million cells/24 h and remained relatively stable at later passages (3.54 and 2.87 ng/million/24 h, respectively, for passages 2 and 5 after blasticidin selection), which indicated integration of the BMP2 gene into the genome (Fig. 5B). The nontransduced hMDSC supernatant had no ELISA-detectable BMP2. AP staining, performed after blasticidin selection, revealed that the lenti-BMP2-transduced hMDSCs did not increase AP expression (Fig. 5C). In vitro multipotent differentiation indicated that the lenti-BMP2-transduced cells exhibited enhanced osteogenic and chondrogenic differentiation, as detected by microCT, von Kossa, osteocalcin, and Alcian blue staining; however, they did not undergo myogenic

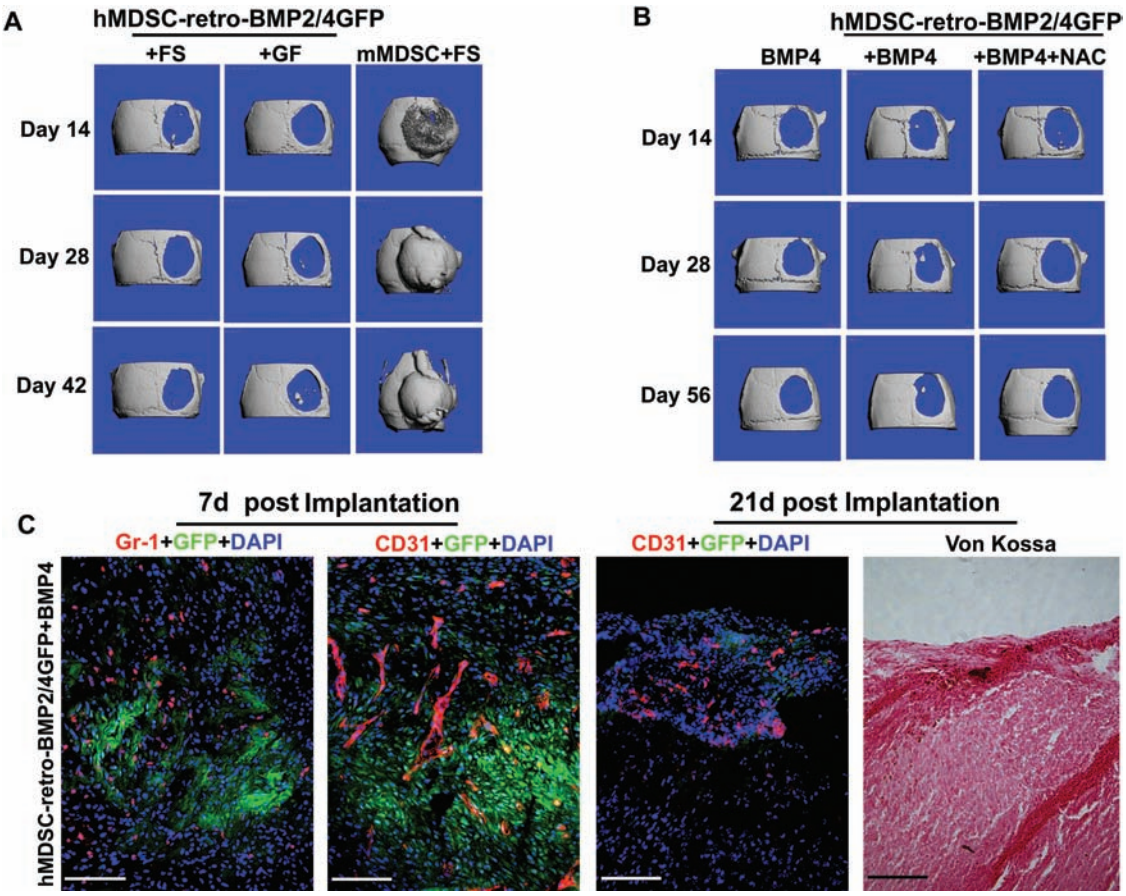

Figure 3. Bone regeneration after transplantation of retro-BMP2/4GFP-transduced hMDSCs. (A) No bone formation was detected by microCT within the defect area at 42 days after the transplantation of retro-BMP2/4GFP-transduced hMDSCs using either fibrin sealant (FS) or Gelfoam (GF) in B6 severe combined immunodeficient (SCID) mice. Complete defect healing was observed 4 weeks after the transplantation of retro-BMP4GFP-transduced mMDSCs (mMDSC + FS). (B) No bone regeneration was observed after transplantation of BMP4 stimulation (+BMP4) or NAC treatment plus BMP4 (+BMP4+NAC) retro-BMP2/4GFP-transduced hMDSCs in CBSCBG SCID (SCID beige) mice at any time point. (C) Many GFP-positive donor cells (green), granulocyte receptor-1 (Gr-1)-positive host neutrophils (red), and vascular endothelial cells (red) were found at the defect site 1 week postimplantation, but only a very few GFP-positive cells were detected after 3 weeks. Only isolated spots of mineralization were identified in the defect area as shown by von Kossa staining (black) at 21 days. Scale bar: 100 μm. DAPI, 4′,6-diamidino-2-phenylindole, dihydrochloride.

differentiation (Fig. 5D, E). The mRNA expression of SOX-9, BMPR1b, BMPR2, and COX-2 did not change after lenti-BMP2 transduction (Fig. 5F).

Lenti-BMP2-Transduced hMDSCs Induced Calvarial Bone Regeneration in CD-1 Nude Mice

We transplanted the retro-BMP2/4GFP-transduced hMDSCs and lenti-BMP2-transduced hMDSCs into a critical-sized calvarial bone defect created in CD-1 nude mice using fibrin sealant as a scaffold and monitored bone formation by microCT biweekly. There was no bone formation at any time point in the control group that received scaffold alone. The retro-BMP2/4GFP-transduced hMDSCs were also unable to induce bone formation in the calvarial defect in these animals. In contrast, bone regeneration was detected as early as 2 weeks after surgery in the lenti-BMP2-transduced hMDSC group (hMDSC-lenti-BMP2) (Fig. 6A). Quantification of the newly regenerated bone area and volume revealed nearly complete defect coverage (approximately 80%) and markedly greater volume of new bone in the defect area in the lenti-BMP2-transduced hMDSC group compared to the other two groups (Fig. 6B and C). Two-dimensional microCT images obtained in the coronal plane at 6 weeks postimplantation showed that the regenerated bone had native bone-like structural characteristics and was well integrated into the surrounding host bone (Fig. 7A). Herovici's staining demonstrated that the newly regenerated bone in the lenti-BMP2-transduced hMDSC group contained mainly type I collagen-rich bone matrix (red), which was similar to the native bone seen on

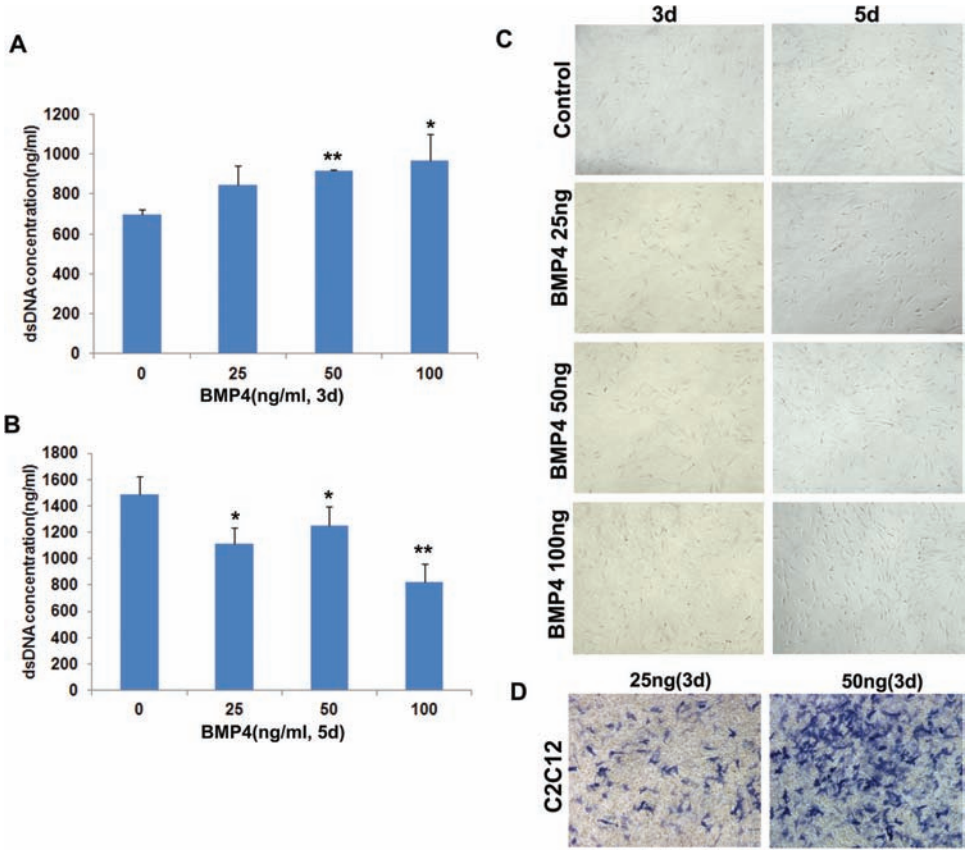

Figure 4. The effect of BMP4 protein stimulation on hMDSC proliferation in vitro. (A) hMDSC proliferation increased after 3 days when 50 or 100 ng/ml of BMP4 was added to the culture medium on day 1. (B) hMDSC proliferation decreased after 5 days when BMP4 was added on days 1 and 3 using three different dosages (25, 50, or 100 ng/ml). $*p < 0.05$, $**p < 0.01$ compared to the untreated controls. $n = 4$ in each treatment group. (C) hMDSCs did not express alkaline phosphatase (AP) after BMP4 stimulation at 3 or 5 days. Scale bars: 200 μm. (D) C2C12 cells expressed AP after BMP4 stimulation for 3 days. Scale bars: 200 μm. dsDNA, double-stranded DNA.

the contralateral side of the defect. The defects in the scaffold control and retro-BMP2/4GFP-transduced hMDSC (hMDSC-retro-BMP2/4GFP) groups displayed mainly granulation tissue composed of type III collagen (blue) (Fig. 7B, C). The transplantation of three other hMDSC populations transduced with lenti-BMP2 demonstrated similar results (data not shown). A significant amount of new bone was detected in all the animals that received different populations of lenti-BMP2-transduced hMDSCs, although the BMP2 secretion levels among the different hMDSC populations varied from 0.303 to 1.219 ng/million cells/24 h.

DISCUSSION

The emerging techniques in regenerative medicine using the combination of stem cell transplantation and gene therapy are very promising and, in the near future, may become suitable for clinical application. Skeletal muscle is a readily available source of adult stem cells, and several investigators have reported that human muscle-derived cells exhibit mesenchymal stem cell characteristics and are capable of differentiating into multiple mesodermal phenotypes (adipogenic, chondrogenic, and osteogenic) in vitro (17,24,29,41,45,46). Human muscle-derived cells have also been shown to form bone and cartilage in vivo (31).

Our previous studies demonstrated that cells isolated from human skeletal muscle and transduced with adeno-BMP2 or retro-BMP2 could promote ectopic bone formation and heal critical-sized calvarial defects created in SCID mice (25,33). The cell populations used in the above studies were mostly cells that would adhere to the flasks within 5 days after initial plating. These cells were considered to be a mixture of fibroblasts, myoblasts, and other muscle progenitor cells. In the current study, we used a modified preplate technique to isolate muscle-derived stem cells from human skeletal muscle, the same technique that has been successfully used to isolate murine muscle-derived stem cells (14). The cells we defined as hMDSCs are the floating cells that do not adhere after 5 days of culture and eventually adhered

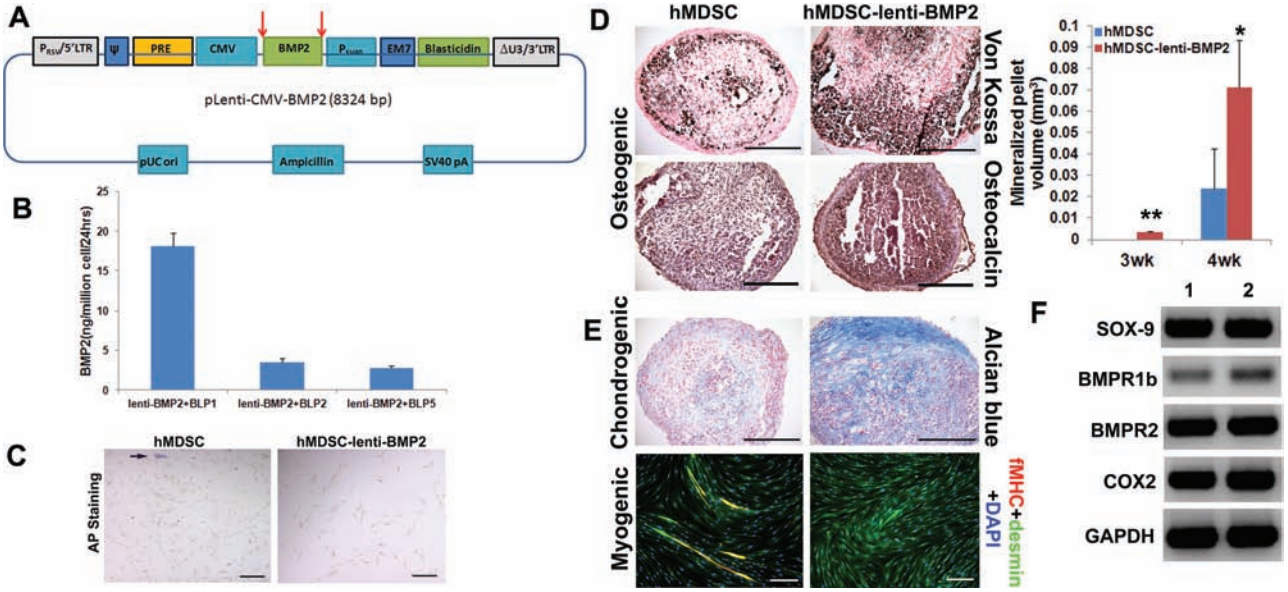

Figure 5. BMP2 secretion levels and in vitro multipotent differentiation of hMDSC after lenti-BMP2 transduction. (A) Schematic illustration of the lenti-BMP2 vector. Red arrows indicate insertion sites of the target BMP2 gene. (B) BMP2 secretion after hMDSC transduction and selection with blasticidin at passages 1, 2, and 5. (C) AP staining showed no increase in AP-positive cell (arrow) number after hMDSC transduction with lenti-BMP2. (D) Osteogenic differentiation was enhanced after transduction of hMDSCs with lenti-BMP2 as shown by von Kossa staining, osteocalcin immunohistochemistry, and microCT. (E) Lenti-BMP2 transduction enhanced chondrogenic differentiation but prevented from myogenic differentiation. (F) RT-PCR indicated no significant change in osteogenic-related genes after lenti-BMP2 transduction. Scale bars: 200 μm. BLP, passage after blasticidin selection.

to the collagen-coated flask after an extended period of time (slow-adhering cells). The morphology of the hMDSCs that we isolated using this technique were mesenchymal stem (stromal) cell-like (flat and fibroblast-like in appearance), which is quite different from the murine MDSCs, which are usually small and round. Characterization of the hMDSCs by flow cytometry showed that the cells were nearly homogeneous in terms of their expression of the myogenic marker CD56, the pericyte/endothelial marker CD146, and more than 99% of the hMDSCs expressed the classical mesenchymal stem cell markers CD73, CD90, CD105, and CD44. These cells were negative for the hematopoietic stem cell marker CD45 and the endothelial cell marker UEA-1R. The in vitro multipotent differentiation assays we performed demonstrated that the hMDSCs could differentiate into adipogenic, chondrogenic, osteogenic, and myogenic lineages. These results suggested that the hMDSCs we isolated were likely mesenchymal stem cells of muscle origin, according to the criteria set out by the International Society of Cell Therapy (10). Slowly adhering hMDSCs have already been shown to possess a better cardiac repair ability in comparison to fast-adhering cells (35). In order to promote the application of hMDSCs in clinic for bone defect healing, we further investigated the osteogenic differentiation capacity of the hMDSCs in combination with BMP4 and BMP2 gene therapy.

Retro-BMP2/4-transduced mMDSCs have been shown to be capable of inducing bone formation and promoting calvarial defect healing (37,38); therefore, we tested whether hMDSCs transduced with retro-BMP2/4GFP could also induce bone formation and promote bone healing. We found that both nontransduced hMDSCs and the retro-BMP2/4GFP-transduced hMDSCs were capable of undergoing osteogenic differentiation in vitro, although the BMP2/4GFP-transduced cells formed larger mineralized pellets. Furthermore, we found that the hMDSCs endogenously expressed the BMP2/4 receptors *BMPR1B* and *BMPR2*, as well as *SOX-9* and *COX-2*, which are involved in endochondral bone formation (1,19,22,34); however, when the retro-BMP2/4GFP-transduced hMDSCs were transplanted into a calvarial defect created in SCID mice, they did not induce bone formation within the defect using either fibrin sealant or Gelfoam scaffolds. There could be several explanations for the hMDSCs' failure to form bone in vivo including host immune rejection, insufficient BMP4 secretion levels by the transduced cells, and/or rapid cell death after transplantation. Although B6 SCID mice are deficient in T lymphocytes, they still possess macrophages, NK cells, and B lymphocytes; therefore, we utilized an alternative recipient animal strain, C.B-Igh-1b/GbmsTAC-PrkdcSCID mice (SCID beige mice), which are deficient in T lymphocytes,

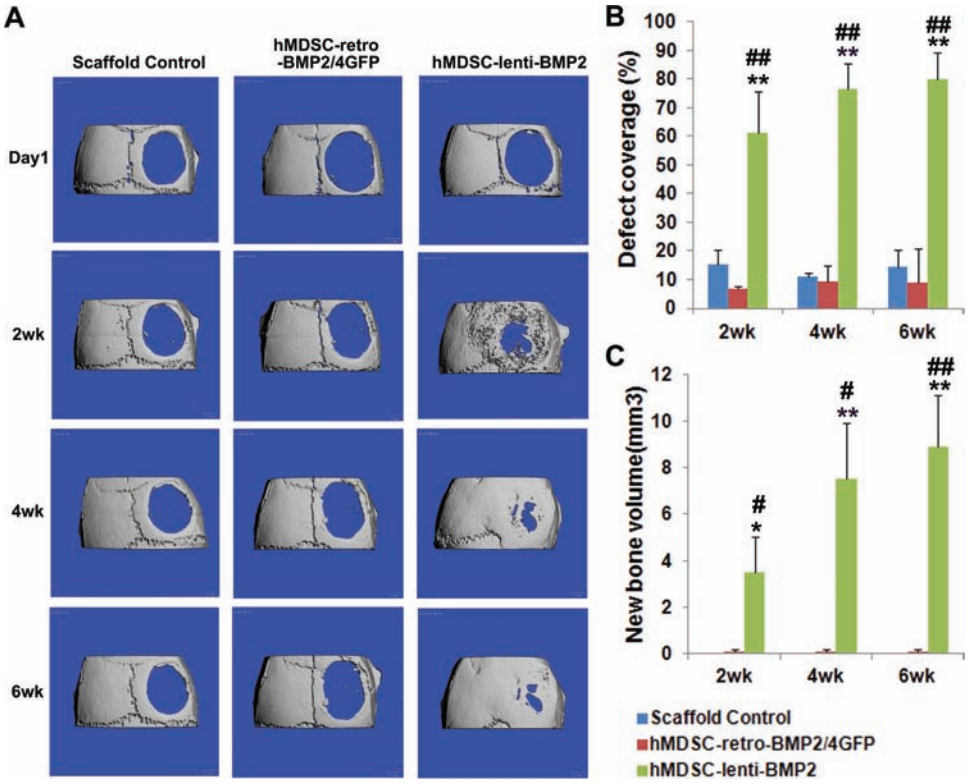

Figure 6. Bone regeneration after transplantation of lenti-BMP2-transduced hMDSCs. (A) MicroCT images of the different treatment groups showed negligible bone formation in the retro-BMP2/4GFP-transduced hMDSCs (hMDSC-retro-BMP2/4GFP) and scaffold control groups. In contrast, robust bone formation was observed in the lenti-BMP2-transduced hMDSC (hMDSC-lenti-BMP2) group at 2 weeks, and nearly complete defect healing was detected by 6 weeks. (B) Quantification of the calvarial defect area covered by the regenerated bone after 6 weeks showed 80%, 10%, and 14% healing in the hMDSC-lenti-BMP2 group, hMDSC-retro-BMP2/4GFP, and scaffold control groups, respectively. (C) Quantification of the regenerated bone volume after 6 weeks showed significantly more bone in the hMDSC-lenti-BMP2 group compared to the other groups, $^{**}p < 0.01$, compared to scaffold control, $^{\#\#}p < 0.01$, compared to the hMDSC-retro-BMP2/4GFP group.

NK cells, and macrophages in order to examine the role of host immune rejection in our future experiments. The inability of the retro-BMP2/4GFP-transduced hMDSCs to induce bone could also be due to the lower amount of BMP4 secreted by the hMDSCs compared to the BMP4 secreted by the retro-BMP2/4-transduced mMDSCs previously reported (37); however, local application of BMP4 protein into the defect area during surgery did not enhance bone formation. Lastly, the lack of in vivo bone formation could be related to rapid death of the hMDSCs after transplantation; therefore, we attempted to improve the survival of the hMDSCs by treating them with NAC before transplantation. It has been reported that mMDSCs treated with NAC were capable of improving heart function after cardiac infarction in comparison to untreated cells (11); once again, no improvement in bone formation was observed when the NAC-treated cells were transplanted into the same calvarial defect model. Unfortunately, all these latter attempts to enhance bone formation using the retro-BMP2/4GFP-transduced hMDSCs failed, even in SCID beige mice after 8 weeks.

There are very few reports indicating that BMP4 can promote human adult stem cell-mediated bone regeneration. BMP4 has been shown to be incapable of promoting endosteal bone formation mediated by stem cell antigen-1 positive (SCA-1$^+$) cells transduced with lenti-BMP2/4 and administered via retro-orbital injection in C57BL/6J mice that underwent sublethal irradiation (15) and could only induce mesenchymal stem cells to undergo osteogenic differentiation under low-serum conditions (7). It has also been demonstrated that low doses of BMP4 (0.01–0.1 ng/ml) could increase human adipose stem cell proliferation and maintain their "stemness," while high doses of BMP4 (10–100 ng) had adverse effects (44). The fact that the proliferation of bone marrow-derived mesenchymal stem cells was also inhibited in the presence of higher concentrations of BMP4 (100 ng/ml) (12) raised our suspicion that BMP4 may also have adverse effects on hMDSCs.

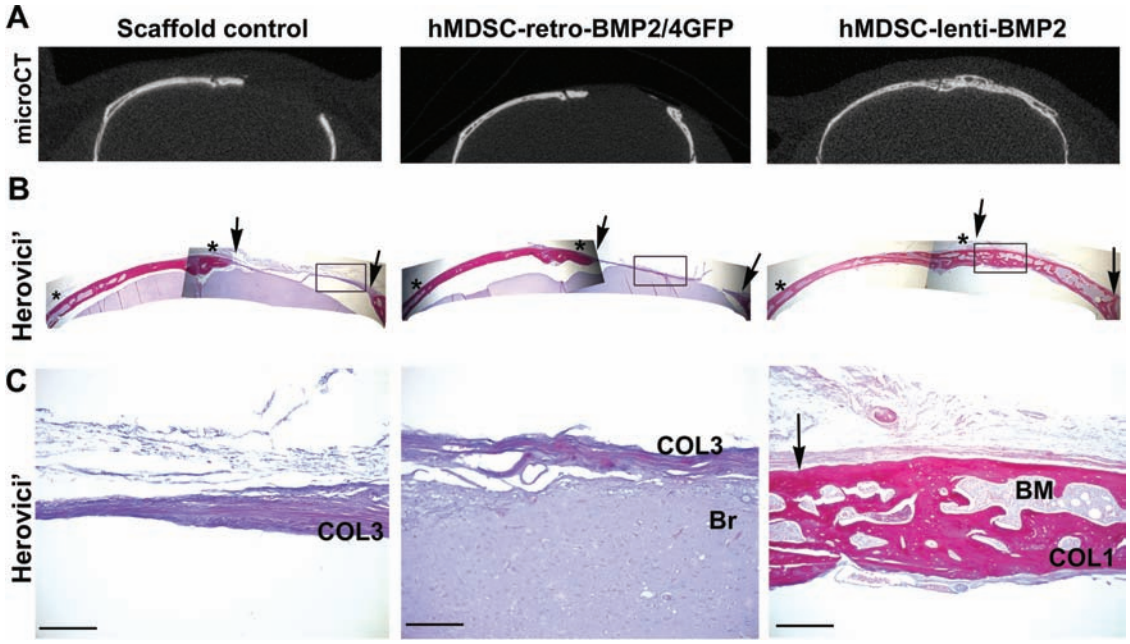

Figure 7. Morphometric and histological characteristics of the newly regenerated calvarial bone. (A) MicroCT demonstrated that the regenerated bone in the hMDSC-lenti-BMP2 group was similar to the native bone and was well integrated into the surrounding host bone. (B) Herovici's staining of cross sections of skull tissues (20×) showing that the regenerated bone (the area between arrows indicate calvarial defect region) in the hMDSC-lenti-BMP2 group was similar to the native bone in the contralateral side (area between stars). (C) Higher magnification (200×) of the regenerated bone area (box area in B) showing that hMDSC-lenti-BMP2 group contained mainly type I collagen (red) and was well integrated with the host bone (arrow). The tissue within the defect in scaffold control and hMDSC-retro-BMP2/4GFP groups mainly consisted of type III collagen (blue). Scale bars: 100 μm. COL1, type I collagen; COL3, type III collagen; Br, brain; BM, bone marrow.

Indeed, our in vitro results demonstrated that prolonged BMP4 stimulation inhibited hMDSC proliferation. On the other hand, it is also possible that the transplanted hMDSCs may be subjected to competing environmental signals from the host, such as BMP2 signaling. It has been reported that BMP2, secreted from the host dura mater, can accelerate human adipose-derived stromal cell-mediated bone regeneration (28). In our case, the retro-BMP2/4-transduced cells secreted BMP4, while the host dura mater secreted BMP2; hence, these two proteins may compete for the BMP-binding sites of the receptors (BMPR1b and BMPR2) responsible for osteogenic differentiation of the hMDSCs. Therefore, we concluded that the proper selection of growth factors plays an important role in human stem cell-mediated bone formation.

Lentiviral vectors are human cell specific and randomly integrate into the cells' genome, which is similar to the retroviral vector, and therefore, this virus can promote long-term exogenous gene expression by the transduced cells. Lentiviral vectors are also superior to retroviral vectors because they infect both dividing and nondividing cells and usually do not require multiple rounds of infection. It has been shown in a rat posterolateral spine fusion model that lenti-BMP2-transduced rat bone marrow cells resulted in spinal fusion, but no fusion was observed using nontransduced and lenti-GFP-transduced cells (32). Lentiviral vectors have been used to transduce human bone marrow stem cells to express several different growth factors (13). We constructed a lentiviral vector, carrying the human BMP2 gene and efficiently transduced the hMDSCs, which had no effect on their proliferation capacity after cell transduction. Although BMP2 secretion decreased after selection with blasticidin, it continued to be secreted at relatively stable levels (2.87 ng/million cells/24 h) during several consecutive passages. In addition, the hMDSCs did not express AP after lenti-BMP2 transduction indicating that the cells remained undifferentiated; however, when they were transplanted into a calvarial defect in CD-1 mice, they formed new bone as early as 2 weeks and almost completely healed the defect by 6 weeks. We also have evidence that other hMDSC populations, which secrete even less BMP2, can form similar amounts of new bone in vivo (unpublished data). These results indicated that appropriate levels of BMP2 secretion are required and that induction of bone formation can occur even at BMP2 concentrations as low as 0.303 ng/million cells/24 h. Moreover, the newly formed bone was found well integrated into the surrounding native bone as shown by microCT and histology.

In conclusion, our study indicates that hMDSCs isolated by the preplate technique are most likely mesenchymal stem cells of muscle origin. BMP2 was found to be far superior to BMP4 in terms of promoting the bone regenerative capacity of hMDSCs in vivo. Moreover, the strain of the host mice did not significantly influence the bone regenerative capacity of the hMDSCs, provided they were immunodeficient. Finally, we demonstrate that the bone formation capacity of the hMDSCs is not affected by the cell scaffolds used in this study (Gelfoam and fibrin sealant), although other scaffolds may. We believe these findings provide valuable insights for future investigations of human muscle-derived stem cell-mediated bone regeneration in clinical applications.

ACKNOWLEDGMENTS: We thank Deanna L. Rhoads from Dr. Stephen Badylak's Laboratory, McGowan Institute of Regenerative Medicine, University of Pittsburgh for performing the Herovici's staining. We also thank Alison Logar from the Children's Hospital of Pittsburgh for flow cytometry cell sorting and analysis and appreciate Dr. Burhan Gharaibeh's help in formatting the references. This project was supported by an NIH grant to Dr. Johnny Huard (NIH 5RO1-DE13420-09). Dr. Johnny Huard receives remuneration as a consultant and royalties from Cook Myosite Inc. All the other authors have no potential conflict of interest to disclose.

REFERENCES

1. Akiyama, H.; Chaboissier, M. C.; Martin, J. F.; Schedl, A.; de Crombrugghe, B. The transcription factor Sox9 has essential roles in successive steps of the chondrocyte differentiation pathway and is required for expression of Sox5 and Sox6. J. Bone. Miner. Res. 17:S142–S142; 2002.
2. Behr, B.; Tang, C.; Germann, G.; Longaker, M. T.; Quarto, N. Locally applied vascular endothelial growth factor A increases the osteogenic healing capacity of human adipose-derived stem cells by promoting osteogenic and endothelial differentiation. Stem Cells 29(2):286–296; 2011.
3. Bouxsein, M. L.; Boyd, S. K.; Christiansen, B. A.; Guldberg, R. E.; Jepsen, K. J.; Muller, R. Guidelines for assessment of bone microstructure in rodents using micro-computed tomography. J. Bone. Miner. Res. 25(7):1468–1486; 2010.
4. Chou, Y. F.; Zuk, P. A.; Chang, T. L.; Benhaim, P.; Wu, B. M. Adipose-derived stem cells and BMP2: Part 1. BMP2-treated adipose-derived stem cells do not improve repair of segmental femoral defects. Connect. Tissue Res. 52(2):109–118; 2011.
5. Chuang, C. K.; Lin, K. J.; Lin, C. Y.; Chang, Y. H.; Yen, T. C.; Hwang, S. M.; Sung, L. Y.; Chen, H. C.; Hu, Y. C. Xenotransplantation of human mesenchymal stem cells into immunocompetent rats for calvarial bone repair. Tissue Eng. Part A 16(2):479–488; 2010.
6. Connolly, J. F.; Guse, R.; Tiedeman, J.; Dehne, R. Autologous marrow injection as a substitute for operative grafting of tibial nonunions. Clin. Orthop. Relat. Res. (266):259–270; 1991.
7. Cordonnier, T.; Langonne, A.; Sohier, J.; Layrolle, P.; Rosset, P.; Sensebe, L.; Deschaseaux, F. Consistent osteoblastic differentiation of human mesenchymal stem cells with bone morphogenetic protein 4 and low serum. Tissue Eng. Part C Methods 17(3):249–259; 2011.
8. Cowan, C. M.; Shi, Y. Y.; Aalami, O. O.; Chou, Y. F.; Mari, C.; Thomas, R.; Quarto, N.; Contag, C. H.; Wu, B.; Longaker, M. T. Adipose-derived adult stromal cells heal critical-size mouse calvarial defects. Nat. Biotechnol. 22(5):560–567; 2004.
9. Crisan, M.; Yap, S.; Casteilla, L.; Chen, C. W.; Corselli, M.; Park, T. S.; Andriolo, G.; Sun, B.; Zheng, B.; Zhang, L.; Norotte, C.; Teng, P. N.; Traas, J.; Schugar, R.; Deasy, B. M.; Badylak, S.; Buhring, H. J.; Giacobino, J. P.; Lazzari, L.; Huard, J.; Peault, B. A perivascular origin for mesenchymal stem cells in multiple human organs. Cell Stem Cell 3(3):301–313; 2008.
10. Dominici, M.; Le Blanc, K.; Mueller, I.; Slaper-Cortenbach, I.; Marini, F.; Krause, D.; Deans, R.; Keating, A.; Prockop, D.; Horwitz, E. Minimal criteria for defining multipotent mesenchymal stromal cells. The International Society for Cellular Therapy position statement. Cytotherapy 8(4):315–317; 2006.
11. Drowley, L.; Okada, M.; Beckman, S.; Vella, J.; Keller, B.; Tobita, K.; Huard, J. Cellular antioxidant levels influence muscle stem cell therapy. Mol. Ther. 18(10):1865–1873; 2010.
12. Farre, J.; Roura, S.; Prat-Vidal, C.; Soler-Botija, C.; Llach, A.; Molina, C. E.; Hove-Madsen, L.; Cairo, J. J.; Godia, F.; Bragos, R.; Cinca, J.; Bayes-Genis, A. FGF-4 increases in vitro expansion rate of human adult bone marrow-derived mesenchymal stem cells. Growth Factors 25(2):71–76; 2007.
13. Fierro, F. A.; Kalomoiris, S.; Sondergaard, C. S.; Nolta, J. A. Effects on proliferation and differentiation of multipotent bone marrow stromal cells engineered to express growth factors for combined cell and gene therapy. Stem Cells 29(11):1727–1737; 2011.
14. Gharaibeh, B.; Lu, A.; Tebbets, J.; Zheng, B.; Feduska, J.; Crisan, M.; Peault, B.; Cummins, J.; Huard, J. Isolation of a slowly adhering cell fraction containing stem cells from murine skeletal muscle by the preplate technique. Nat. Protoc. 3(9):1501–1509; 2008.
15. Hall, S. L.; Chen, S. T.; Gysin, R.; Gridley, D. S.; Mohan, S.; Lau, K. H. Stem cell antigen-1+ cell-based bone morphogenetic protein-4 gene transfer strategy in mice failed to promote endosteal bone formation. J. Gene Med. 11(10):877–888; 2009.
16. Hernigou, P.; Poignard, A.; Beaujean, F.; Rouard, H. Percutaneous autologous bone-marrow grafting for nonunions. Influence of the number and concentration of progenitor cells. J. Bone Joint Surg. Am. 87(7):1430–1437; 2005.
17. Jackson, W. M.; Aragon, A. B.; Djouad, F.; Song, Y.; Koehler, S. M.; Nesti, L. J.; Tuan, R. S. Mesenchymal progenitor cells derived from traumatized human muscle. J. Tissue Eng. Regen. Med. 3(2):129–138; 2009.
18. James, A. W.; Levi, B.; Nelson, E. R.; Peng, M.; Commons, G. W.; Lee, M.; Wu, B.; Longaker, M. T. Deleterious effects of freezing on osteogenic differentiation of human adipose-derived stromal cells in vitro and in vivo. Stem Cells Dev. 20(3):427–439; 2011.
19. Jeon, J.; Oh, H.; Lee, G.; Ryu, J. H.; Rhee, J.; Kim, J. H.; Chung, K. H.; Song, W. K.; Chun, C. H.; Chun, J. S. Cytokine-like 1 knock-out mice (Cytl1−/−) show normal cartilage and bone development but exhibit augmented osteoarthritic cartilage destruction. J. Biol. Chem. 286(31):27206–27213; 2011.
20. Jeon, O.; Rhie, J. W.; Kwon, I. K.; Kim, J. H.; Kim, B. S.; Lee, S. H. In vivo bone formation following transplantation of human adipose-derived stromal cells that

are not differentiated osteogenically. Tissue Eng. Part A 14(8):1285–1294; 2008.
21. Kim, J.; Kim, I. S.; Cho, T. H.; Lee, K. B.; Hwang, S. J.; Tae, G.; Noh, I.; Lee, S. H.; Park, Y.; Sun, K. Bone regeneration using hyaluronic acid-based hydrogel with bone morphogenic protein-2 and human mesenchymal stem cells. Biomaterials 28(10):1830–1837; 2007.
22. Kim, J. S.; Ryoo, Z. Y.; Chun, J. S. Cytokine-like 1 (Cytl1) regulates the chondrogenesis of mesenchymal cells. J. Biol. Chem. 282(40):29359–29367; 2007.
23. Kitoh, H.; Kitakoji, T.; Tsuchiya, H.; Mitsuyama, H.; Nakamura, H.; Katoh, M.; Ishiguro, N. Transplantation of marrow-derived mesenchymal stem cells and platelet-rich plasma during distraction osteogenesis—A preliminary result of three cases. Bone 35(4):892–898; 2004.
24. Lecourt, S.; Marolleau, J. P.; Fromigue, O.; Vauchez, K.; Andriamanalijaona, R.; Ternaux, B.; Lacassagne, M. N.; Robert, I.; Boumediene, K.; Chereau, F.; Marie, P.; Larghero, J.; Fiszman, M.; Vilquin, J. T. Characterization of distinct mesenchymal-like cell populations from human skeletal muscle in situ and in vitro. Exp. Cell Res. 316(15):2513–2526; 2010.
25. Lee, J. Y.; Peng, H.; Usas, A.; Musgrave, D.; Cummins, J.; Pelinkovic, D.; Jankowski, R.; Ziran, B.; Robbins, P.; Huard, J. Enhancement of bone healing based on ex vivo gene therapy using human muscle-derived cells expressing bone morphogenetic protein 2. Hum. Gene Ther. 13(10):1201–1211; 2002.
26. Levame, M.; Meyer, F. Herovici's picropolychromium. Application to the identification of type I and III collagens. Pathol. Biol. 35(8):1183–1188; 1987.
27. Levi, B.; James, A. W.; Nelson, E. R.; Vistnes, D.; Wu, B.; Lee, M.; Gupta, A.; Longaker, M. T. Human adipose derived stromal cells heal critical size mouse calvarial defects. PLoS One 5(6):e11177; 2010.
28. Levi, B.; Nelson, E. R.; Li, S.; James, A. W.; Hyun, J. S.; Montoro, D. T.; Lee, M.; Glotzbach, J. P.; Commons, G. W.; Longaker, M. T. Dura mater stimulates human adipose-derived stromal cells to undergo bone formation in mouse calvarial defects. Stem Cells 29(8):1241–1255; 2011.
29. Levy, M. M.; Joyner, C. J.; Virdi, A. S.; Reed, A.; Triffitt, J. T.; Simpson, A. H.; Kenwright, J.; Stein, H.; Francis, M. J. Osteoprogenitor cells of mature human skeletal muscle tissue: An in vitro study. Bone 29(4):317–322; 2001.
30. Lin, L.; Shen, Q.; Wei, X.; Hou, Y.; Xue, T.; Fu, X.; Duan, X.; Yu, C. Comparison of osteogenic potentials of BMP4 transduced stem cells from autologous bone marrow and fat tissue in a rabbit model of calvarial defects. Calcif. Tissue Int. 85(1):55–65; 2009.
31. Mastrogiacomo, M.; Derubeis, A. R.; Cancedda, R. Bone and cartilage formation by skeletal muscle derived cells. J. Cell. Physiol. 204(2):594–603; 2005.
32. Miyazaki, M.; Sugiyama, O.; Tow, B.; Zou, J.; Morishita, Y.; Wei, F.; Napoli, A.; Sintuu, C.; Lieberman, J. R.; Wang, J. C. The effects of lentiviral gene therapy with bone morphogenetic protein-2-producing bone marrow cells on spinal fusion in rats. J. Spinal. Disord. Tech. 21(5):372–379; 2008.
33. Musgrave, D. S.; Pruchnic, R.; Bosch, P.; Ziran, B. H.; Whalen, J.; Huard, J. Human skeletal muscle cells in ex vivo gene therapy to deliver bone morphogenetic protein-2. J. Bone Joint Surg. Br. 84(1):120–127; 2002.
34. Naik, A. A.; Xie, C.; Zuscik, M. J.; Kingsley, P.; Schwarz, E. M.; Awad, H.; Guldberg, R.; Drissi, H.; Puzas, J. E.; Boyce, B.; Zhang, X.; O'Keefe, R. J. Reduced COX-2 expression in aged mice is associated with impaired fracture healing. J. Bone Miner. Res. 24(2):251–264; 2009.
35. Okada, M.; Payne, T. R.; Drowley, L.; Jankowski, R. J.; Momoi, N.; Beckman, S.; Chen, W. C.; Keller, B. B.; Tobita, K.; Huard, J. Human skeletal muscle cells with a slow adhesion rate after isolation and an enhanced stress resistance improve function of ischemic hearts. Mol. Ther. 20(1):138–145; 2012.
36. Peng, H.; Chen, S. T.; Wergedal, J. E.; Polo, J. M.; Yee, J. K.; Lau, K. H.; Baylink, D. J. Development of an MFG-based retroviral vector system for secretion of high levels of functionally active human BMP4. Mol. Ther. 4(2):95–104; 2001.
37. Peng, H.; Wright, V.; Usas, A.; Gearhart, B.; Shen, H. C.; Cummins, J.; Huard, J. Synergistic enhancement of bone formation and healing by stem cell-expressed VEGF and bone morphogenetic protein-4. J. Clin. Invest. 110(6):751–759; 2002.
38. Peng, H. R.; Usas, A.; Olshanski, A.; Ho, A. M.; Gearhart, B.; Cooper, G. M.; Huard, J. VEGF improves, whereas sFlt1 inhibits, BMP2-induced bone formation and bone healing through modulation of angiogenesis. J. Bone Miner. Res. 20(11):2017–2027; 2005.
39. Pieraggi, M. T.; Julian, M.; Bouissou, H.; Stocker, S.; Grimaud, J. A. Dermal aging. Immunofluorescence study of collagens I and III and fibronectin. Ann. Pathol. 4(3):185–194; 1984.
40. Quarto, R.; Mastrogiacomo, M.; Cancedda, R.; Kutepov, S. M.; Mukhachev, V.; Lavroukov, A.; Kon, E.; Marcacci, M. Repair of large bone defects with the use of autologous bone marrow stromal cells. N. Engl. J. Med. 344(5):385–386; 2001.
41. Sinanan, A. C.; Hunt, N. P.; Lewis, M. P. Human adult craniofacial muscle-derived cells: Neural-cell adhesion-molecule (NCAM; CD56)-expressing cells appear to contain multipotential stem cells. Biotechnol. Appl. Biochem. 40(Pt 1):25–34; 2004.
42. Tiedeman, J. J.; Garvin, K. L.; Kile, T. A.; Connolly, J. F. The role of a composite, demineralized bone matrix and bone marrow in the treatment of osseous defects. Orthopedics 18(12):1153–1158; 1995.
43. Turner, N. J.; Pezzone, M. A.; Brown, B. N.; Badylak, S. F. Quantitative multispectral imaging of Herovici's polychrome for the assessment of collagen content and tissue remodelling. J. Tissue. Eng. Regen. Med. 7(2):139–148; 2013.
44. Vicente Lopez, M. A.; Vazquez Garcia, M. N.; Entrena, A.; Olmedillas Lopez, S.; Garcia-Arranz, M.; Garcia-Olmo, D.; Zapata, A. Low doses of bone morphogenetic protein 4 increase the survival of human adipose-derived stem cells maintaining their stemness and multipotency. Stem Cells Dev. 20(6):1011–1019; 2011.
45. Wada, M. R.; Inagawa-Ogashiwa, M.; Shimizu, S.; Yasumoto, S.; Hashimoto, N. Generation of different fates from multipotent muscle stem cells. Development 129(12):2987–2995; 2002.
46. Williams, J. T.; Southerland, S. S.; Souza, J.; Calcutt, A. F.; Cartledge, R. G. Cells isolated from adult human skeletal muscle capable of differentiating into multiple mesodermal phenotypes. Am. Surg. 65(1):22–26; 1999.
47. Zheng, B.; Cao, B.; Crisan, M.; Sun, B.; Li, G.; Logar, A.; Yap, S.; Pollett, J. B.; Drowley, L.; Cassino, T.; Gharaibeh, B.; Deasy, B. M.; Huard, J.; Peault, B. Prospective identification of myogenic endothelial cells in human skeletal muscle. Nat. Biotechnol. 25(9):1025–1034; 2007.